KeAi
CHINESE ROOTS
GLOBAL IMPACT

Available online at www.sciencedirect.com

ScienceDirect

Advances in Climate Change Research 10 (2019) 250–263

www.keaipublishing.com/en/journals/accr/

Sensitivity of the simulated CO_2 concentration to inter-annual variations of its sources and sinks over East Asia

FU Yu[a,*], LIAO Hong[b], TIAN Xiang-Jun[c], GAO Hao[d], CAI Zhao-Nan[e], HAN Rui[c]

[a] *Climate Change Research Center, Chinese Academy of Sciences, Beijing, 100029, China*
[b] *Jiangsu Key Laboratory of Atmospheric Environment Monitoring and Pollution Control, Jiangsu Collaborative Innovation Center of Atmospheric Environment and Equipment Technology, School of Environmental Science and Engineering, Nanjing University of Information Science and Technology, Nanjing, 210044, China*
[c] *International Center for Climate and Environment Sciences, Institute of Atmospheric Physics, Chinese Academy of Sciences, Beijing, 10029, China*
[d] *National Satellite Meteorological Center, China Meteorological Administration, Beijing, 100081, China*
[e] *Key Laboratory of Middle Atmosphere and Global Environment Observation, Institute of Atmospheric Physics, Chinese Academy of Sciences, Beijing, 10029, China*

Received 30 October 2019; revised 19 February 2020; accepted 9 March 2020
Available online 20 March 2020

Abstract

The study on how the variations in CO_2 sources and sinks can affect the CO_2 concentration over East Asia would be useful to provide information for policymaker concerning carbon emission reduction. In this study, a nested-grid version of global chemical transport model (GEOS-Chem) is employed to assess the impacts of variations in meteorological parameters, terrestrial fluxes, fossil fuel emissions, and biomass burning on inter-annual variations of CO_2 concentrations over East Asia in 2004–2012. Simulated CO_2 concentrations are compared with observations at 14 surface stations from the World Data Centre for Greenhouse Gases (WDCGG) and satellite-derived CO_2 column density (X_{CO_2}) from the Gases Observing SATellite (GOSAT). The comparison shows that the simulated CO_2 column density is generally higher than that of GOSAT by 1.33×10^{-6} (annual mean point by point biases averaged over East Asia). The model reasonably captures the temporal variations of CO_2 concentrations observed at the ground-based stations, but it is likely to underestimate the peaks-to-troughs amplitude of the seasonal cycle by 50% or more. The simulated surface CO_2 concentration in East Asia exhibits the largest inter-annual variation in December-January–February (DJF). The regional mean absolute deviation (MAD) values over East Asia are within $(4.4–5.0) \times 10^{-6}$ for all seasons. Model sensitivity simulations indicate that the inter-annual variations of surface CO_2 concentrations are mainly driven by variations of meteorological parameters, and partly modulated by the inter-annual variations of terrestrial fluxes and fossil fuel emissions in local regions. The variations of the terrestrial fluxes and fossil fuel emissions may account for ~28% of the inter-annual variation of surface CO_2 concentration in southern China. The inter-annual variations of the peaks-to-troughs amplitude are dependent on variations of meteorological parameters, terrestrial fluxes and fossil fuel emissions in local regions. The influence of biomass burning emissions is relatively weak.

Keywords: Carbon dioxide; Inter-annual variation; Terrestrial biosphere flux; Fossil fuel emission

1. Introduction

Carbon dioxide (CO_2) is one of the most important long-lived greenhouse gases in the atmosphere. Its spatio-temporal variations are affected by human activities (i.e., fossil fuel consumption, cement production, and land use change), as well as the exchanges between atmosphere and biosphere/ocean. East Asia, especially China, has been developing rapidly in the past few decades, accompanied by increased anthropogenic emissions. The atmospheric CO_2 levels in China hit new highs (up to 407×10^{-6}) in 2017, with a relatively high annual growth rate due to large anthropogenic emissions (CMA, 2018). The terrestrial ecosystems in East

* Corresponding author.
E-mail address: fuyu@mail.iap.ac.cn (FU Y.).
Peer review under responsibility of National Climate Center (China Meteorological Administration).

https://doi.org/10.1016/j.accre.2020.03.001

Asia might play a critical role in the regional carbon budget (Le Quéré et al., 2018). However, there still exist large uncertainties in the magnitude and spatio-temporal pattern of terrestrial carbon sinks at continental and regional scales resulted from the complex interactions between biosphere and atmosphere (Piao et al., 2009a, 2009b; Zhang et al., 2014; Jiang et al., 2016; Thompson et al., 2016). With rising scientific and political concerns about the regional effects of the carbon cycle, it is very essential to understand the high-resolution CO_2 spatial distribution and variation of CO_2, and a more objective estimate for the impact of the carbon flux on the CO_2 concentration variations in East Asia may help the policymakers about the carbon emission reduction and climate adaptation.

Chemical transport model (CTM) is a common tool for studying the variation of atmospheric CO_2 concentrations at global/regional scale. The CO_2 volume fraction in CTM is driven by prior inputs of CO_2 fluxes, including fossil fuel emission, biofuel emission, biomass burning emission, oceanic and terrestrial fluxes etc., and mediated by atmospheric transport. In order to investigate the spatio-temporal variation of the CO_2 concentration, many studies focused on evaluating the applicability of chemical transport models in CO_2 simulations by using atmospheric CO_2 ground-based observations as well as satellite-based CO_2 column density (X_{CO_2}) measurements (Feng et al., 2011; Zhang et al., 2015; Li et al., 2017). For instance, Feng et al. (2011) assessed the global chemical transport model (GEOS-Chem) simulation of CO_2 by using surface observations, aircraft measurements and satellite data from Atmospheric Infrared Sounder (AIRS) during 2003−2006. In East Asia, Li et al. (2017) evaluated the regional chemical model (CMAQ) simulation of the CO_2 concentration in 2012 by using GOSAT observations and ground measurements. However, due to the large uncertainties in regional carbon sources and sinks, the performance of high-resolution CTM in simulating the spatio-temporal variation of CO_2 remains unclear, especially the inter-annual variation over East Asia.

Some efforts have been made to investigate the contribution of terrestrial ecosystems to the atmospheric CO_2 concentration based on chemical model simulations. Randerson et al. (1997) and Nevison et al. (2008) indicated that the terrestrial flux contributes 40%−80% to both seasonal and inter-annual variations of CO_2 in the Northern Hemisphere. However, the contribution of terrestrial ecosystems to the CO_2 concentration is contingent on the prescribed terrestrial carbon flux in the model. Several studies have analyzed the impacts of the terrestrial flux uncertainty on the CO_2 concentration, and the results showed that large discrepancies in the prescribed terrestrial flux could lead to biases over 5×10^{-6} in the CO_2 concentration near surface (Fujita et al., 2003; Chen et al., 2013; Messerschmidt et al., 2013).

The data assimilation using CTM model system and observations offers a good way to provide optimized CO_2 fluxes. Therefore, some works of CO_2 simulations have tried to use the optimized estimates of terrestrial fluxes derived from the data assimilation systems to reduce the uncertainties associated with terrestrial fluxes (Nassar et al., 2010; Feng et al., 2011; Deng and Chen, 2011; Kou et al., 2015). Only a few studies focused on East Asia. Kou et al. (2015) reported that terrestrial fluxes could elevate the CO_2 concentration in North China and Southeast China in winter (December−February, DJF) by over 5×10^{-6} while reduce it by over 7×10^{-6} in summer (June−August, JJA) by using a regional CTM (RAMS-CMAQ) with and without terrestrial fluxes in East Asia. Nevertheless, the contribution of terrestrial ecosystems to the inter-annual variation of the atmospheric CO_2 concentration over East Asia has not been addressed in most modeling studies. In addition, excluding of the inter-annual variation of terrestrial fluxes might be an important source of uncertainties for further carbon flux assimilation, since the terrestrial fluxes have been reported to exhibit a significant inter-annual variation because of the changes in meteorological parameters (e.g., temperature and precipitation), land cover and land use (Zeng et al., 2005; Piao et al., 2009a; Sitch et al., 2015; Wang et al., 2016).

In this study, a comprehensive CO_2 simulation in East Asia during 2004−2012 is conducted by using a nested version of global chemical transport model with the optimized terrestrial fluxes from CarbonTracker. The main goals of this study are to investigate the variation of atmospheric CO_2 concentration, and to quantify impacts of the major CO_2 sources and sinks on the atmospheric CO_2 concentration at both seasonal and inter-annual scales, which helps to better understand the carbon sources and sinks, as well as regulate the carbon emissions.

2. Methods and data

2.1. Methods

2.1.1. Model description

The CO_2 concentration over East Asia (11°S−55°N, 70°−150°E) is simulated by using the nested grid global chemical transport model (GEOS-Chem v10-01, http://www.geos-chem.org), which is driven by the GEOS-5 assimilated meteorological fields from the Goddard Earth Observing System (GEOS) of the NASA Global Modeling and Assimilation Office. The nested GEOS-Chem model has a horizontal resolution of 0.5° latitude by 0.667° longitude and 47 vertical layers. The chemical boundary conditions are taken from the GEOS-Chem global simulations performed at the horizontal resolution of 2° latitude × 2.5° longitude. The GEOS-Chem simulation of CO_2 has been previously used in the forwards simulations of CO_2 (Shim et al., 2011; Cogan et al., 2012; Chen et al., 2013) and inversion studies (Feng et al., 2009; Nassar et al., 2011; Deng et al., 2014). The GEOS-Chem CO_2 simulation is developed by Suntharalingam et al. (2004), and further undated by Nassar et al. (2010). In this study, the CO_2 is transported as a tracer with the prior CO_2 fluxes from fossil fuel combustion and cement production, biomass burning, biofuel burning, ocean exchanges, terrestrial exchanges, shipping, aviation and chemical productions from the oxidation of carbon monoxide, as well as methane and non-methane volatile organic compounds.

2.1.2. Numerical experiments

The following CO_2 simulations from 2004 to 2012 are conducted to identify the contributions of variations in emissions and meteorological parameters to the seasonal and inter-annual variations of CO_2 in East Asia. As suggested by Nassar et al. (2010), our model simulations are initialized on January 1st, 2003, with a globally uniform CO_2 field of 373.71×10^{-6} that based on the monthly mean sea surface CO_2 concentration at Mauna Loa Observatory in Hawaii from NOAA-ESRL. After one year spin-up simulation from this initialized state, a more realistic initial distribution of atmospheric CO_2 in January 2004 is derived and used to drive all the simulations.

VAll is the control simulation with variations in meteorological parameters, fossil fuel emissions, biomass burning emissions, terrestrial fluxes, and ocean fluxes from 2004 to 2012. Boundary conditions for CO_2 are updated from the coupled global VAll simulations performed at the horizontal resolution of 2° latitude × 2.5° longitude. VMet is the simulation with changes in meteorological parameters during 2004−2012, while fossil fuel emissions, biomass burning emissions, terrestrial fluxes and ocean fluxes are fixed at the 2004 level. Boundary conditions for this nested sensitivity simulations are taken from the coupled global VMET simulations performed at the horizontal resolution 2° latitude × 2.5° longitude. VTer is the simulation with changes in terrestrial fluxes during 2004−2012 over East Asia, while meteorological parameters, fossil fuel emissions, biomass burning emissions and ocean fluxes are fixed at the 2004 level. VFF is the simulation with changes in fossil fuel emissions during 2004−2012 over East Asia, while meteorological parameters, biomass burning emissions, terrestrial fluxes and ocean fluxes are fixed at the 2004 level. VBB is the simulation with changes in biomass burning emission during 2004−2012 over East Asia, while meteorological parameters, fossil fuel emission, terrestrial flux and ocean flux are fixed at the 2004 level. The boundary conditions for the nested sensitivity simulations of VTer, VFF and VBB are taken from the coupled global VAll simulations performed at the horizontal resolution 2° latitude × 2.5° longitude for 2004. It should be noted that the inter-annual variations in meteorological parameters can influence the CO_2 concentration in two ways. First, CO_2 fluxes vary with meteorological parameters. Second, variations of meteorological parameters can influence the CO_2 transport. The sensitivity simulation VMet is performed to examine the sensitivity of CO_2 to inter-annual variations of transport that induced by changes in meteorological parameters. The effects of climate-driven changes in the CO_2 sources and sinks (e.g., terrestrial fluxes, oceanic fluxes, biomass burning) are included in those priori flux data.

2.1.3. Analysis method

To analyze the inter-annual variations of CO_2, we quantify the impact of variations in CO_2 emissions and meteorological parameters on inter-annual variations of the atmospheric CO_2 concentration near surface by using the mean absolute deviation (MAD) and absolute percent departure from the mean (APDM), respectively, representing the absolute inter-annual variation of the CO_2 concentration (Fu and Liao, 2012; Mu and Liao, 2014).

2.2. Data

2.2.1. Emissions

The global emissions of CO_2 used in GEOS-Chem model are listed in Table 1, including fossil fuel emissions, biomass burning emissions, biofuel burning emissions of CO_2 from heating, cooking and removal of agriculture waste, terrestrial

Table 1
Summary of emission inventories used in GEOS-Chem simulations.

Flux type	Flux data description	Global annual flux averaged over 2004−2012 (Pg C per year)	Reference
Fossil fuel combustion and cement production	Open-source Data Inventory for Atmospheric CO_2 emissions (ODIAC) with monthly and inter-annual variation for 2004−2012	8.41	Oda and Maksyutov (2011)
Biofuel burning	Yevich and Logan annually biofuel burning, which are fixed in year 1995 during the simulation	0.82	Yevich and Logan (2003)
Biomass burning	Global Fire Database (GFED) v4 Emission with daily and inter-annual variation for 2004−2012	1.89	van der Werf et al. (2010)
Terrestrial flux	Carbon Tracker 2015 (3-hourly) with inter-annual variation for 2004−2012	−4.15	Peters et al. (2007)
Ocean flux	Scaled monthly ocean exchange with inter-annual variation for 2004−2012	−2.06	Takahashi et al. (2009)
Shipping emission	Monthly variation of International Comprehensive Ocean-Atmosphere Data Set (ICOADS), which are fixed in year 2004	0.29	Corbett and Koehler (2003, 2004)
Aviation emission	Aviation fuel burn spatial and seasonal distribution from AEIC scaled with global annual CO_2 emission totals calculated from the IEA, which are fixed in year 2005	0.21	Simone et al. (2013) and Olsen et al. (2013)
Chemical source	GEOS-Chem CO_2 chemical source with monthly variation and fixed in year 2004	1.14	Nassar et al. (2010)

flux, ocean flux, the global CO_2 emissions from shipping, aviation emissions, and the chemical source of CO_2 based on CO loss rate. To account for the inter-annual variation of terrestrial fluxes, we update the terrestrial exchanges in the model with the optimized estimations of the terrestrial fluxes at the time resolution 3-hourly and the horizontal resolution of 1° latitude × 1° longitude from the CarbonTracker 2015 (CT2015) (http://carbontracker.noaa.gov; Peters et al., 2007).

2.2.2. Satellite observations

The data from version 7.3 of the GOSAT/ACOS X_{CO_2} Level 2 (GOSAT/ACOS_L2_Lite_FP.7.3) from April 2009 to December 2012 is used, which is processed by using the Atmospheric CO_2 Observations from Space (ACOS) algorithms developed by the Orbiting Carbon Observatory (OCO) team (Osterman et al., 2017). X_{CO_2} is expressed as the number of gas molecules in a column above a unit surface area. GOSAT X_{CO_2} retrievals have previously been evaluated by the comparison with ground-based measurements of X_{CO_2} from the Total Carbon Column Observing Network (TCCON) stations (Wunch et al., 2011a; Lindqvist et al., 2015; Kulawik et al., 2016). The validations against TCCON sites data have shown that the mean bias between ACOS and TCCON data is less than 1.5×10^{-6} (Wunch et al., 2011b). Compared with GOSAT X_{CO_2} retrievals, the simulated CO_2 volume mixing ratios are converted to $X_{co_2\_mod}$ at the corresponding time and locations of the observations following the method of Connor et al. (2008) as follows.

$$X_{co_2\_mod} = X^{a}_{CO_2} + h^{T}A(x - x_a) = h^{T}x_a + h^{T}A(x - x_a) \quad (1)$$

where $X^{a}_{CO_2}$ represents the priori column-averaged dry-air mole fraction, h^{T} represents the transpose of pressure weighting function of GOSAT, A represents the averaging kernel matrix of the GOSAT, x is the modeled vertical profile of CO_2 interpolated at the vertical levels of GOSAT, and x_a is the prior CO_2 profile of GOSAT.

2.2.3. Observed ground-based CO_2 concentrations

We also collected the atmospheric CO_2 observations at 14 sites in East Asia from NOAA Earth System Research Laboratory (ESRL, http://www.esrl.noaa.gov/gmd/ccgg/) and World Data Center for Greenhouse Gases (WDCGG, http://ds.data.jma.go.jp/gmd/wdcgg/), for which measurements are available from 2004 to 2012. A summary of the Asian surface sites used is shown in Table 2, and the geophysical location of those sites and the study domain are shown in Fig. 1.

3. Model evaluation

3.1. Evaluation of terrestrial flux

Here we firstly assessed the spatial and temporal variations in CO_2 sources and sinks for better understanding the model performance in simulating CO_2 concentration. As

Table 2
Summary and statistical characteristics of the simulated and the observed CO_2 concentrations at 14 sites in East Asia.

Site	Lon. (°E)	Lat. (°N)	Altitude (m)	Observation periods	Contributor	CO_2 concentration ($\times 10^{-6}$)							
						Obs	Mod[a]	MB[b]	r[c]	R_{amp}[d]	Mod[e]	MB[f]	r[g]	R_{amp}[h]
Mt.Waliguan (WLG)	100.9	36.3	3810	2004.01–2012.12	CMA, NOAA/ESRL	386.1	386.3	−0.22	0.92	0.42	386.8	−0.72	0.97	0.73
Shangdianzi (SDZ)	117.12	40.65	287	2009.09–2011.12	CMA, NOAA/ESRL	398.2	401.0	−2.76	0.21	0.35	403.1	−4.87	0.49	0.54
Lulin, TaiWan (LLN)	120.87	23.47	2867	2006.08–2013.12	NOAA/ESRL	385.5	384.4	1.08	0.58	0.28	390.6	−5.06	0.90	0.45
Hok Tsui and King's Park, Hong Kong (HK)	114.26; 114.17	22.21; 22.31	60; 65	2010.11–2012.11	HKO	396.8	404.8	−7.97	0.78	0.58	403.5	−6.66	0.84	0.55
Kisai-Saitama (KIS)	139.55	36.08	13	2004.01–2012.12	JMA	392.5	399.2	−6.59	0.50	1.12	397.5	−4.98	0.86	0.96
Mikawa-Ichinomiya (MKW)	137.43	34.85	50	2004.01–2011.03	JMA	399.5	390.2	9.36	0.82	0.54	391.1	8.54	0.58	1.05
Mt. Dodaira-Saitama (DDR)	139.18	36	840	2004.01–2012.12	JMA	390.5	388.8	1.69	0.94	0.51	392.2	−1.79	0.97	1.21
Ryori (RYO)	141.82	39.03	260	2004.01–2012.12	JMA	388.7	390.0	−1.31	0.84	0.45	392.0	−3.26	0.95	1.03
Takayama (TKY)	137.42	36.15	1420	2004.01–2008.12	AIST	386.2	383.7	2.48	0.89	0.59	386.0	0.18	0.96	1.32
Yonagunijima (YON)	123.02	24.47	30	2004.01–2012.12	JMA	388.4	388.5	−0.10	0.95	0.54	390.7	−2.35	0.99	1.12
Anmyeon-do (AMY)	126.32	36.53	47	2004.01–2012.12	KMA	391.6	393.8	−2.24	0.70	0.81	397.5	−5.53	0.92	1.09
Tae-ahn Peninsula (TAP)	126.12	36.72	20	2004.01–2012.12	NOAA/ESRL	391.2	393.7	−2.51	0.60	0.70	394.4	−3.19	0.68	1.22
Gosan (GSN)	126.1	33.17	72	2004.01–2011.12	NIER	392.3	388.6	3.70	0.78	0.69	391.8	0.48	0.88	1.27
Ulaan Uul (UUM)	111.08	44.45	914	2004.01–2012.12	NOAA/ESRL	387.1	387.2	−0.06	0.86	0.40	387.6	−0.49	0.97	1.22

[a] and [e] Model results are from nested (0.5° × 0.667°) simulation VAll and global 2° × 2.5° simulation VAll, respectively.
[b] and [f] Mean bias (MB) from nested VAll and global VAll, respectively.
[c] and [g] r (Pearson correlation coefficient) from nested VAll and global VAll, respectively.
[d] and [h] R_{amp} is the ratio of amplitude between the simulated CO_2 and observed CO_2 from nested VAll and global VAll, respectively.

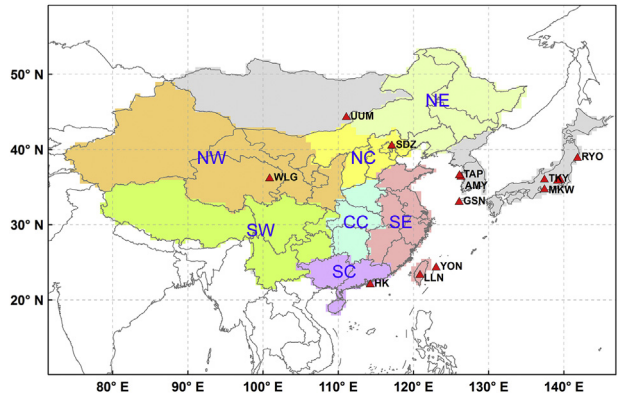

Fig. 1. Geophysical locations of the 14 sites (red triangle) and the regions, including Northeast China (NE), North China (NC), Southeast China (SE), Central China (CC), South China (SC), Southwest China (SW), and Northwest China (NW).

shown in Fig. 2a, the terrestrial fluxes are positive across most of East Asia in winter, indicating the carbon is released from the terrestrial ecosystem to the atmosphere due to the relative weak photosynthesis and strong respiration of vegetation under the cold temperature. While the terrestrial fluxes in summer are negative across East Asia, resulting from the enhanced temperature and radiation. The seasonal distribution pattern of terrestrial fluxes is quite consistent with previous findings (Yu et al., 2013). The annual terrestrial flux shows larger inter-annual variations than fossil fuel emissions, and the biosphere land sink in East Asia increases by 0.11 Pg C per year between 2004−2007 and 2008−2012. This increasing trend of the land sink in East Asia has also been identified in Thompson et al. (2016). For 2004−2012, the mean terrestrial flux of CT2015 in East Asia (China) is −0.62 Pg C per year (−0.53 Pg C per year), which is close to

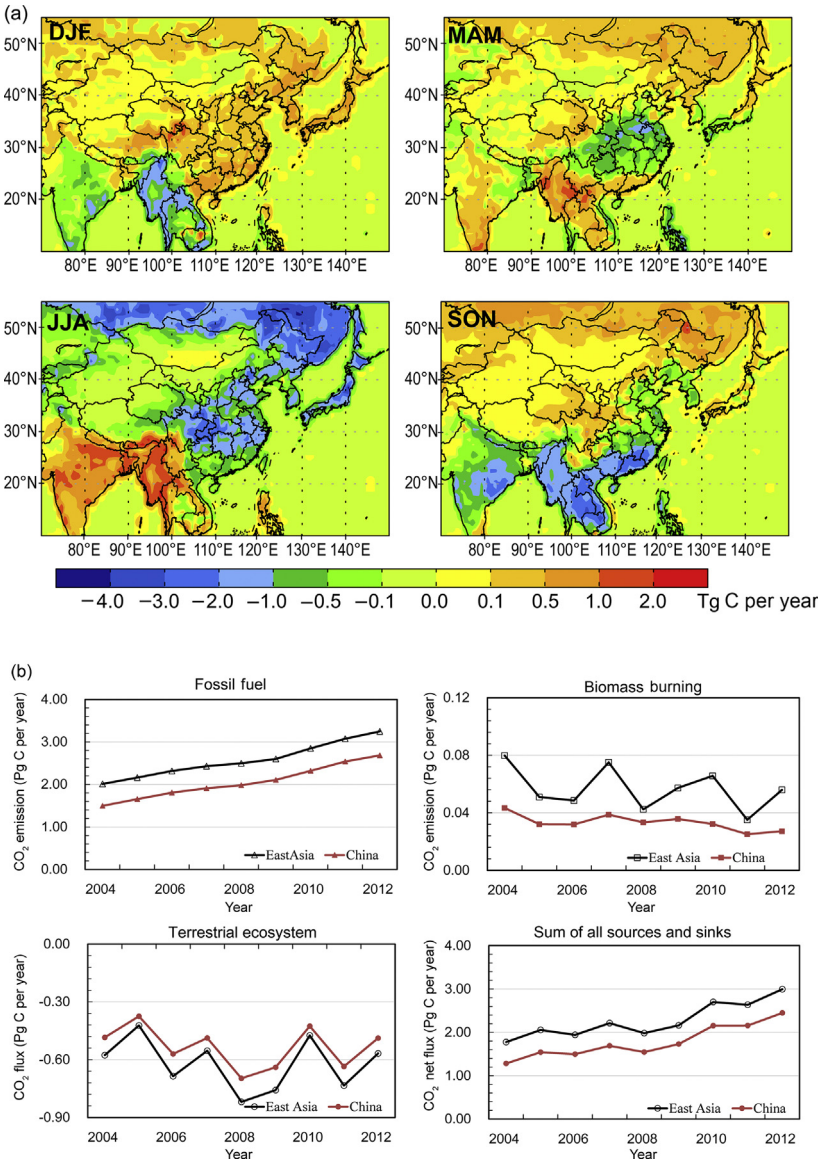

Fig. 2. Horizontal distributions of seasonal mean terrestrial fluxes in winter (December−February, DJF), spring (March−May, MAM), summer (June−August, JJA), and autumn (September−November, SON) of 2004 over East Asia (a); annual CO_2 emissions of fossil fuel, biomass burning and terrestrial ecosystem for 2004−2012 in East Asia and China (b).

the upper limit of Jiang et al. (2016) (Table 3). Overall, the net CO_2 flux over East Asia shows an increasing trend in 2004–2012 (Fig. 2b).

3.2. Comparisons with satellite X_{CO_2} data

The simulated GEOS-Chem X_{CO_2} is compared with the observed GOSAT X_{CO_2} retrievals from April 2009 to December 2012 (Fig. 3). The spatial distributions of the difference between GEOS-Chem X_{CO_2} and GOSAT X_{CO_2} vary seasonally. In DJF and spring (March–May, MAM), the simulated X_{CO_2} concentrations exhibit low biases of -1.0×10^{-6} to -4.0×10^{-6} in North China, North and South Korea, and parts of Japan, but higher biases in some places of South China and Southeast China, which is consistent with the results by Lei et al. (2014). While in summer (JJA) and autumn (September–November, SON), the simulated X_{CO_2} concentrations are generally overestimated in most of East Asia, with the largest high bias up to $(4.0–6.0) \times 10^{-6}$ relative to GOSAT observations in Northeast China. The biases can be mostly attributed to the large uncertainties of the terrestrial flux estimation. The comparison between the terrestrial flux from CT2015 and the observations from eight sites in the Chinese Terrestrial Ecosystem Flux Observation and Research Network (ChinaFLUX) (Yu et al., 2006a, 2006b, 2008, 2013) shows that the terrestrial fluxes of CT2015 fail to reproduce the peak or valley values of the observed terrestrial flux around summer, suggesting that CT2015 might underestimate the CO_2 exchanges between terrestrial ecosystems and the atmosphere. It may represent a CO_2 source and CO_2 sink, depending on the regions. For example, the simulated concentrations are lower than the observations in Southwest China in summer (e.g. Xishuangbanna), and this discrepancy could result from the underestimated terrestrial CO_2 source there. While in Northeast China (e.g. Changbaishan Mountain), the high biases in simulated CO_2 concentrations are likely to occur for the underestimated terrestrial CO_2 sink there (not shown). Previous studies have indicated that the CO_2 exchange between the upper troposphere and lower stratosphere (UTLS) in high latitude and the middle and upper troposphere in subtropical and mid-latitude could impact the CO_2 distribution in DJF and MAM, but the model tends to underestimate CO_2 in the tropical and subtropical upper troposphere and overestimate CO_2 in the extratropical lower stratosphere as the model can't correctly capture the effects of the stratospheric intrusion (Miyazaki et al., 2008; Deng et al., 2015). Hence the discrepancies of CO_2 in the UTLS may partly account for the latitude-dependent biases between the simulated and observed X_{CO_2}. Moreover, the discrepancies between simulated and observed X_{CO_2} are probably due to the overestimated GOSAT X_{CO_2} retrievals over East Asia, which is suggested by Li et al. (2017). Overall, the mean point-by-point biases in DJF, MAM, JJA and SON over the study domain are $(0.82 \pm 1.79) \times 10^{-6}$, $(0.39 \pm 1.50) \times 10^{-6}$, $(2.50 \pm 2.43) \times 10^{-6}$ and $(1.72 \pm 1.65) \times 10^{-6}$ (mean bias ± standard deviation), respectively.

Note that the spatial resolution of the CO_2 fluxes used is lower than the nested model resolution (0.5° latitude × 0.667° longitude). The observed X_{CO_2} is also compared with the simulated X_{CO_2} from global VAll simulations with the model resolution of 2° latitude × 2.5° longitude additionally for assessing the potential impact of the model resolution. As shown in Fig. 3, the spatial distributions of biases between simulations and observations are similar in both high- and low-resolution simulation, but the biases from low-resolution simulations are smaller than those from high-resolution simulations. The differences between the 2° latitude × 2.5° longitude and 0.5° latitude × 0.667° longitude simulations indicates that the biases between the simulated and the observed X_{CO_2} might partly be caused by the downscaling impact of the spatial resolution in the simulation.

Table 3
The terrestrial carbon flux used in this study and that in previous studies.

Citation		Carbon flux (Pg C per year)	Period
Global	Deng and Chen (2011)	−3.63 ± 0.49	2002–2007
	IPCC (2013)	−2.63 ± 1.22	2000–2009
	Le Quéré et al. (2014)	−2.80 ± 0.80	2003–2012
	Poulter et al. (2014)	−3.90 ± 1.30	2011
	Thompson et al. (2016)	−3.17 (−3.65 to −2.28)	2008–2012
	CT2015 (this study)	−5.18	2011
		−4.15	2004–2012
East Asia/Asia	Thompson et al. (2016)	−0.46 (−1.18 to −0.01)	2008–2012
	Zhang et al. (2014)	−1.56 (−1.80 to −1.07)	2006–2010
	CT2015 (this study)	−0.62	2004–2012
China	Zhang et al. (2014)	−0.33 (−0.64 to −0.29)	2001–2010
	Jiang et al. (2016)	−0.45 (−0.51 to −0.39)	2006–2009
	CT2015 (this study)	−0.53	2004–2012

3.3. Comparisons with ground-based measurements

The ability of the GEOS-Chem model to capture the seasonal and inter-annual variations of surface CO_2 is assessed by using the ground-based observations at 14 sites in East Asia from WDCGG. The model exhibits similar inter-annual trends in all the 14 sites. The scatterplots for the simulated and the observed seasonal-mean CO_2 concentrations at 14 stations during 2004–2012 are displayed in Fig. 4. The mean biases of CO_2 concentrations are less than 4.0×10^{-6} in most of the stations except those sites near the urban regions, e.g. HK, KIS and MKW. The relative low correlations (0.21–0.50) at sites of SDZ and KIS as well as the large biases in these sites indicate a difficulty for the model to reproduce the influence of local sources and sinks, especially in the regions of big cities. At the other remote sites, the simulated CO_2 concentrations are consistent with the corresponding observations, with the correlation coefficients between the simulated and observed

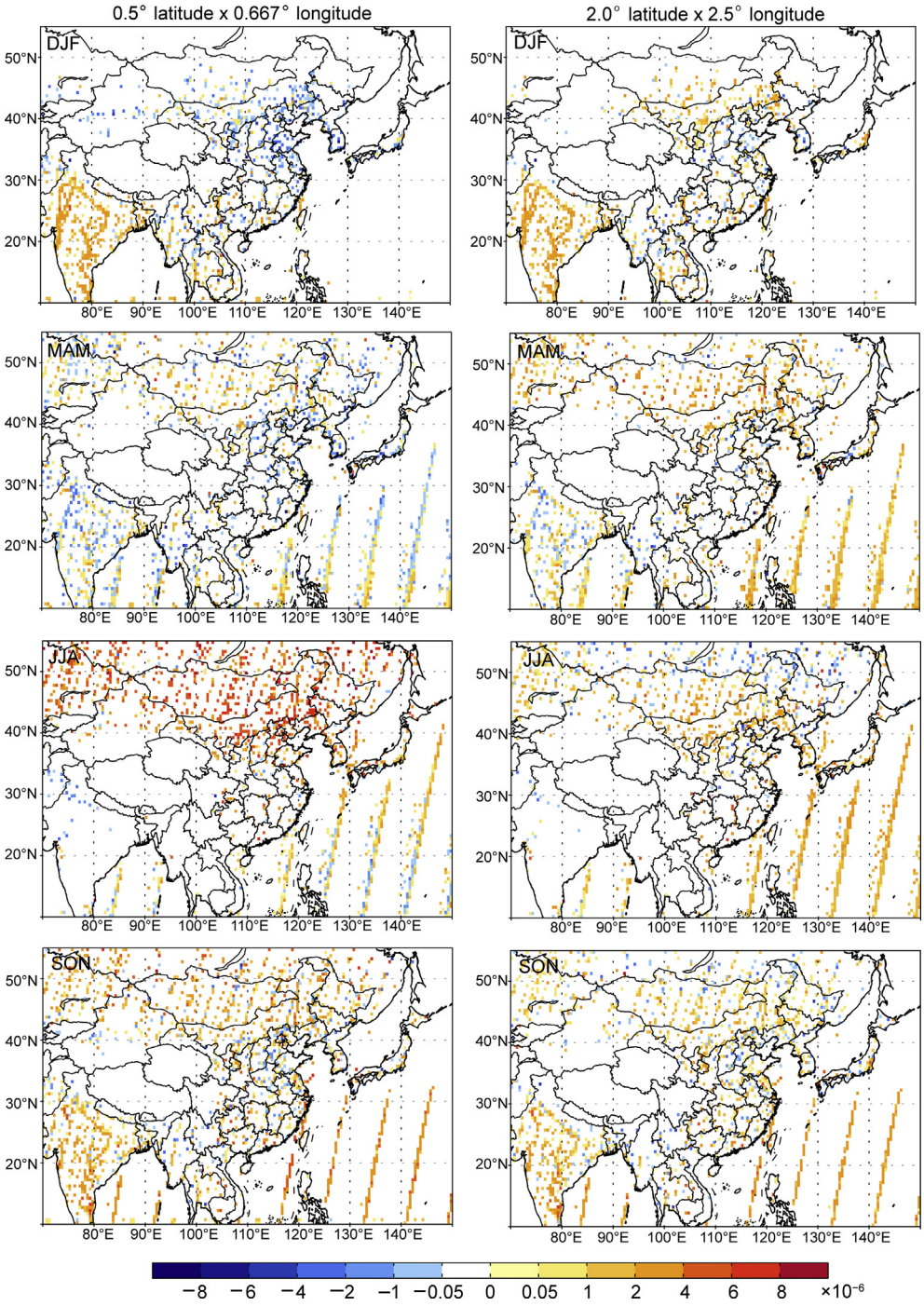

Fig. 3. Biases in the simulated X_{CO_2} (column-averaged dry air mole fraction of CO_2) when model results from 0.5° latitude × 0.667° longitude simulations (left); and from 2.0° latitude × 2.5° longitude simulations (right) are compared with those from GOSAT during Apr. 2009–Dec. 2012, respectively ($X_{co_2\_mod}$ minus $X_{co_2\_sat}$).

CO_2 concentrations ranging from 0.58 (LLN) to 0.95 (YON) (Table 2). The simulated CO_2 concentrations generally show positive biases at most sites (except MKW) in JJA, whereas CO_2 concentrations show a high or low bias in other seasons (Fig. 4). The averaged summertime simulated CO_2 concentration at all sites is 4.1×10^{-6} higher than the observations. It can be inferred that the uncertainties in terrestrial fluxes in JJA may strongly affect the simulated CO_2 concentrations at the locations where the terrestrial biosphere dominates the seasonal cycle. The shape and phasing of the seasonal cycle in the model is overall consistent with those in observations. However, the simulated peaks-to-troughs amplitude of the CO_2 seasonal cycle is smaller than the observed amplitude at most sites, indicating that the GEOS-Chem tends to underestimate the amplitude of the seasonal cycle over East Asia (as inferred from the mean amplitude difference between the simulation

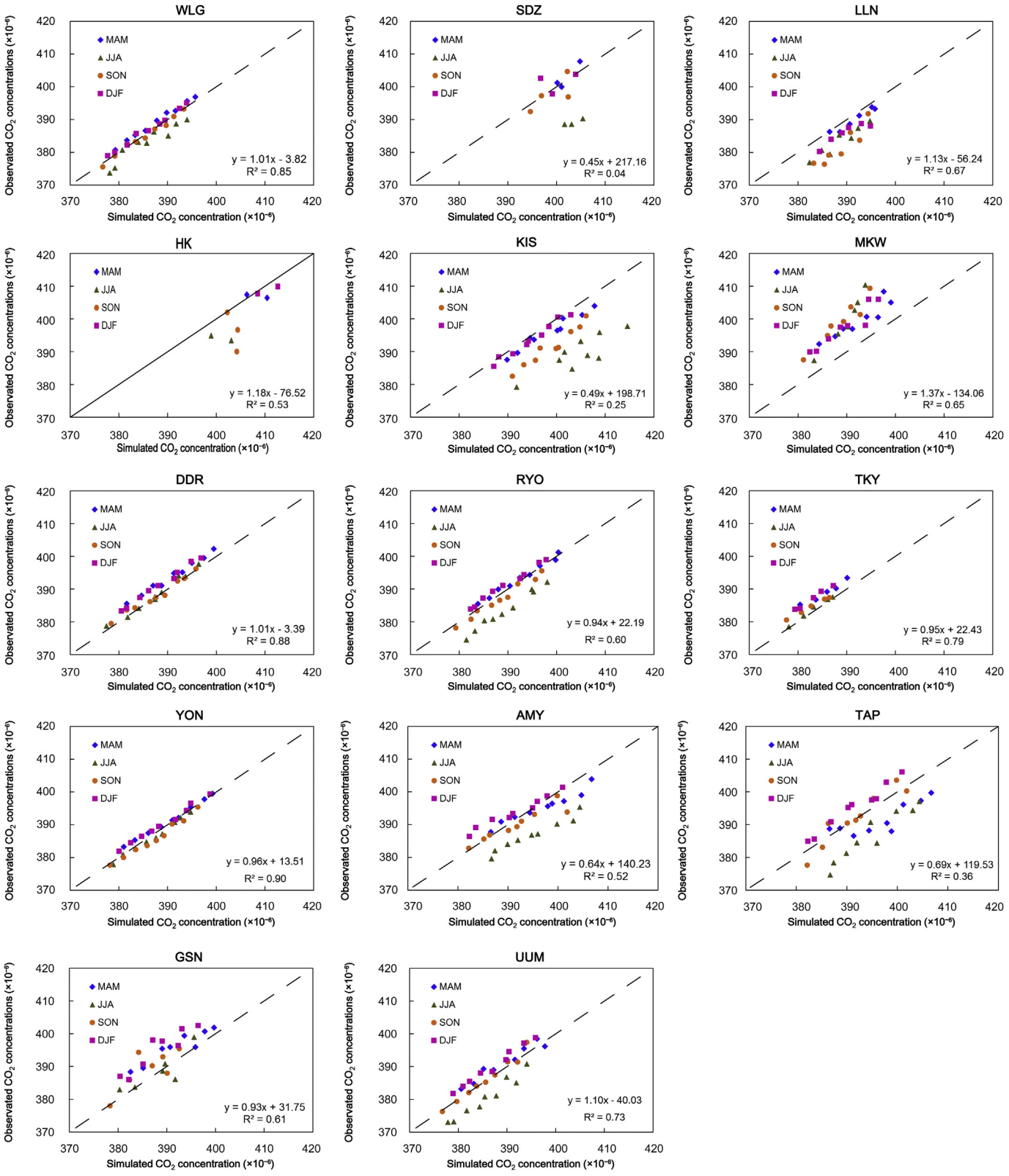

Fig. 4. Comparisons of the simulated seasonal mean surface CO_2 concentrations with the observations at 14 sites for 2004–2012. The 1:1 line is also shown (dashed).

and the observation). The mean value of the ratio between the simulated and observed peaks-to-troughs amplitude show that the simulated amplitude of surface CO_2 concentrations is roughly a half of the observed amplitude. The poorest consistency between the simulated and the observed amplitude appears at LLN and SDZ, where the simulated amplitude

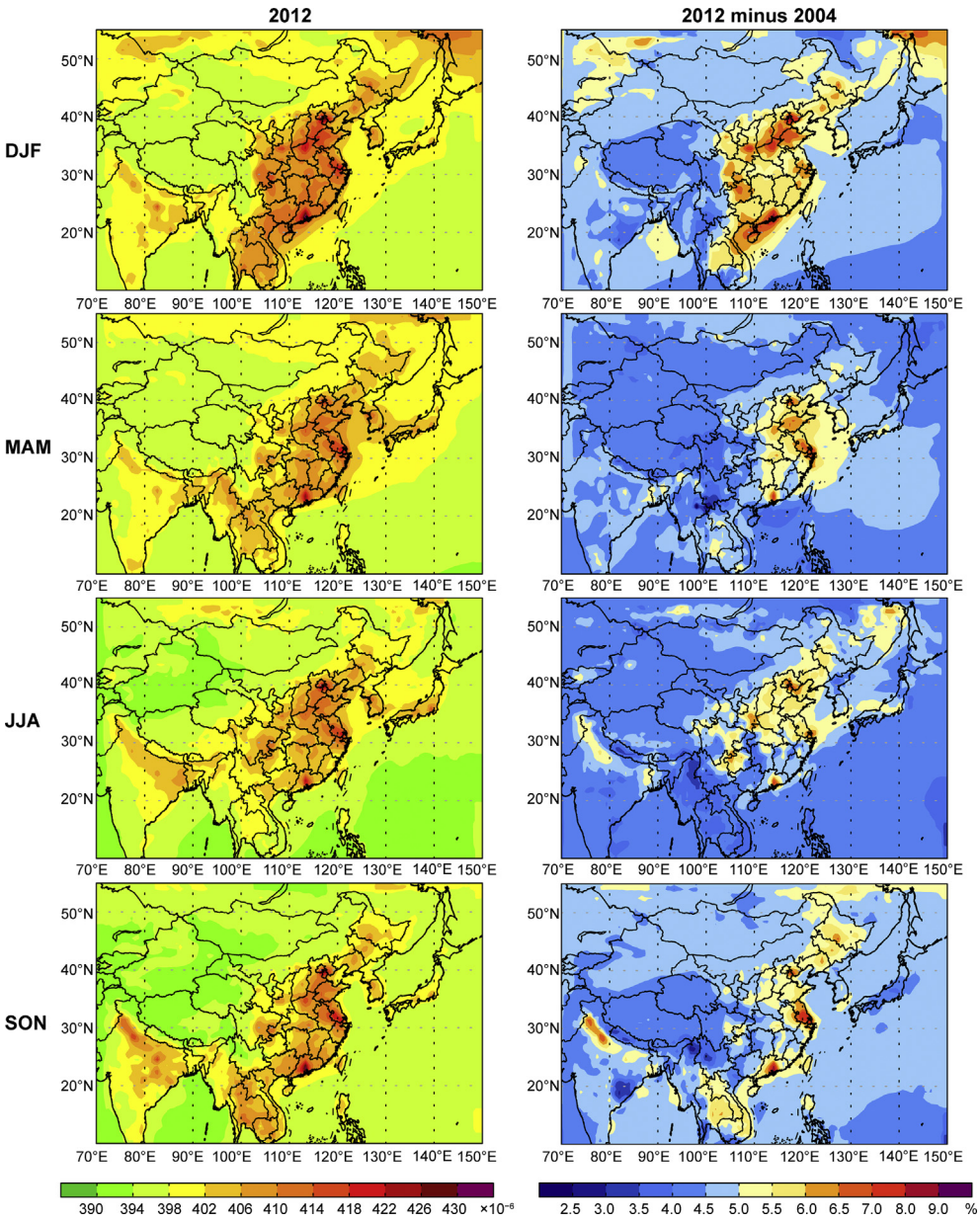

Fig. 5. Horizontal distributions of the simulated surface CO_2 concentration in DJF, MAM, JJA and SON over East Asia for 2012 (left); the percentage changes in the simulated seasonal mean surface CO_2 concentrations in East Asia between 2012 and 2004 (right).

could be one third of the observed amplitude (Table 2). The substantially negative biases between the simulated and the observed amplitudes of the CO_2 seasonal cycle are also noted in previous studies in the Northern Hemisphere (e.g. Nevison et al., 2008). These biases are probably caused by the uncertainties in the prescribed carbon fluxes as discussed above. Also listed in Table 3 are the statistical characteristics of the simulated CO_2 concentrations from the 2° latitude × 2.5° longitude simulation and the observed one. In general, the evaluations of model results indicate that the GEOS-Chem model reasonably captures the spatial distributions and temporal variations of the CO_2 concentration in East Asia despite the biases in the simulated concentration.

4. Simulated changes of CO_2 concentration

4.1. Seasonal mean of CO_2 concentration

The distributions of the simulated seasonal-mean CO_2 concentrations in East Asia for 2012 are shown in Fig. 5. The distributions of the CO_2 concentration are similar in all seasons, and the areas with high CO_2 concentration are consistent with the areas with high anthropogenic CO_2 emissions. High CO_2 concentrations are simulated in East China, with the highest ones in the fairly economically developed areas, such as the Beijing-Tianjin-Hebei regions, the Yangtze River Delta and the Pearl River Delta megacity clusters. The lowest CO_2

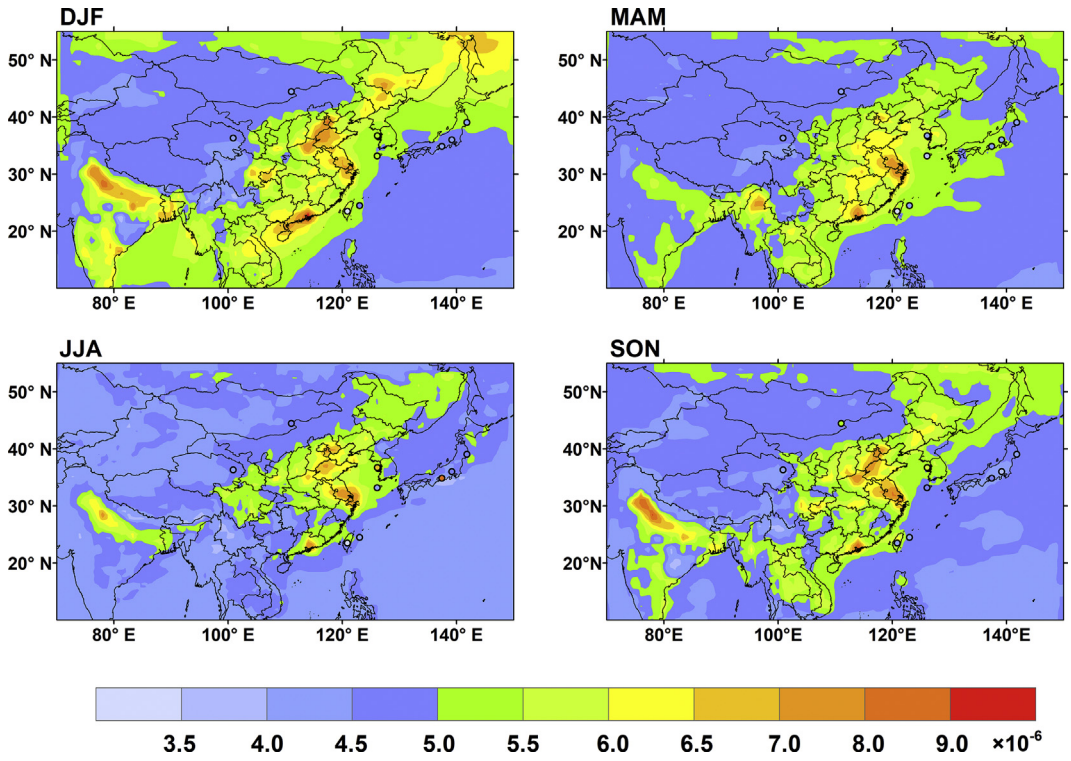

Fig. 6. Mean absolute deviation (MAD) of the simulated surface-layer CO_2 concentrations (shaded) obtained from simulations of VAll during 2004–2012; the MAD values of surface CO_2 concentrations at the observation sites (colored circles).

concentrations exhibit in Northwest China. The simulated CO_2 concentration is the highest in DJF, with the maximum CO_2 concentration exceeding 426×10^{-6} in the Pearl River Delta and the minimum CO_2 concentration below 390×10^{-6} in western China. The CO_2 concentrations in JJA are smaller than the CO_2 concentrations in DJF, which are within the range of $(406–420) \times 10^{-6}$ over East China, Korea and Japan. It is mainly because the terrestrial ecosystems show a higher photosynthesis rate in JJA, and CO_2 is largely absorbed by vegetation during the growing season (Fig. 2a). Also shown in Fig. 5 are the percentage differences of the simulated seasonal-mean surface CO_2 concentrations between 2012 and 2004. We find that the large difference is located in the North China Plain and the Pearl River Delta, with the large increase by ~9% in DJF, which also reflect the increase of CO_2 emissions in those regions during 2004–2012.

4.2. Inter-annual variations of CO_2 concentration

Over 2004–2012, the near-surface annual mean CO_2 concentration in East Asia shows an overall increasing trend ($(2.0–3.0) \times 10^{-6}$ per year). The interannual variations in surface CO_2 over East Asia are shown by MAD values for DJF, MAM, JJA, and SON (Fig. 6). The MAD (APDM) values of the surface CO_2 concentration are also examined based on the measurements in East Asia. It is found that the MAD values of observations vary within the range of $(2.4–8.1) \times 10^{-6}$ in all seasons. Comparisons between the simulated and observed MAD values in East Asia show a good agreement, especially during DJF and SON. In some places in East China where the CO_2 concentration is the highest (e.g. the North China Plain, the Yangtze River Delta, and the Pearl River Delta), the MAD/APDM values obtained from simulation VAll are within $(6.0–9.0) \times 10^{-6}$/(1.8%–2.2%) in all seasons. While the MAD/APDM values over Central China, Northeast China, Northwest China, and Southwest China are within $(4.0–6.0) \times 10^{-6}$/(1.1%–1.8%). The inter-annual variations of the seasonal- and annual-mean surface CO_2 concentrations averaged over different regions in East Asia are summarized in Fig. 7a. The MAD/APDM value of surface CO_2 concentration in simulation VAll is 4.6×10^{-6}/(~1.2%) for annual mean over East Asia.

5. Contribution of the CO_2 fluxes to CO_2 concentration

To understand the inter-annual variations of the surface-layer CO_2 concentration over East Asia, we further analyze the MAD values of seasonal- and annual-mean surface CO_2 concentrations caused by changes in meteorological parameters alone (VMet), variation in terrestrial CO_2 fluxes alone (VTer), variations in fossil fuel emissions alone (VFF), and variations in biomass burning emission alone (VBB),

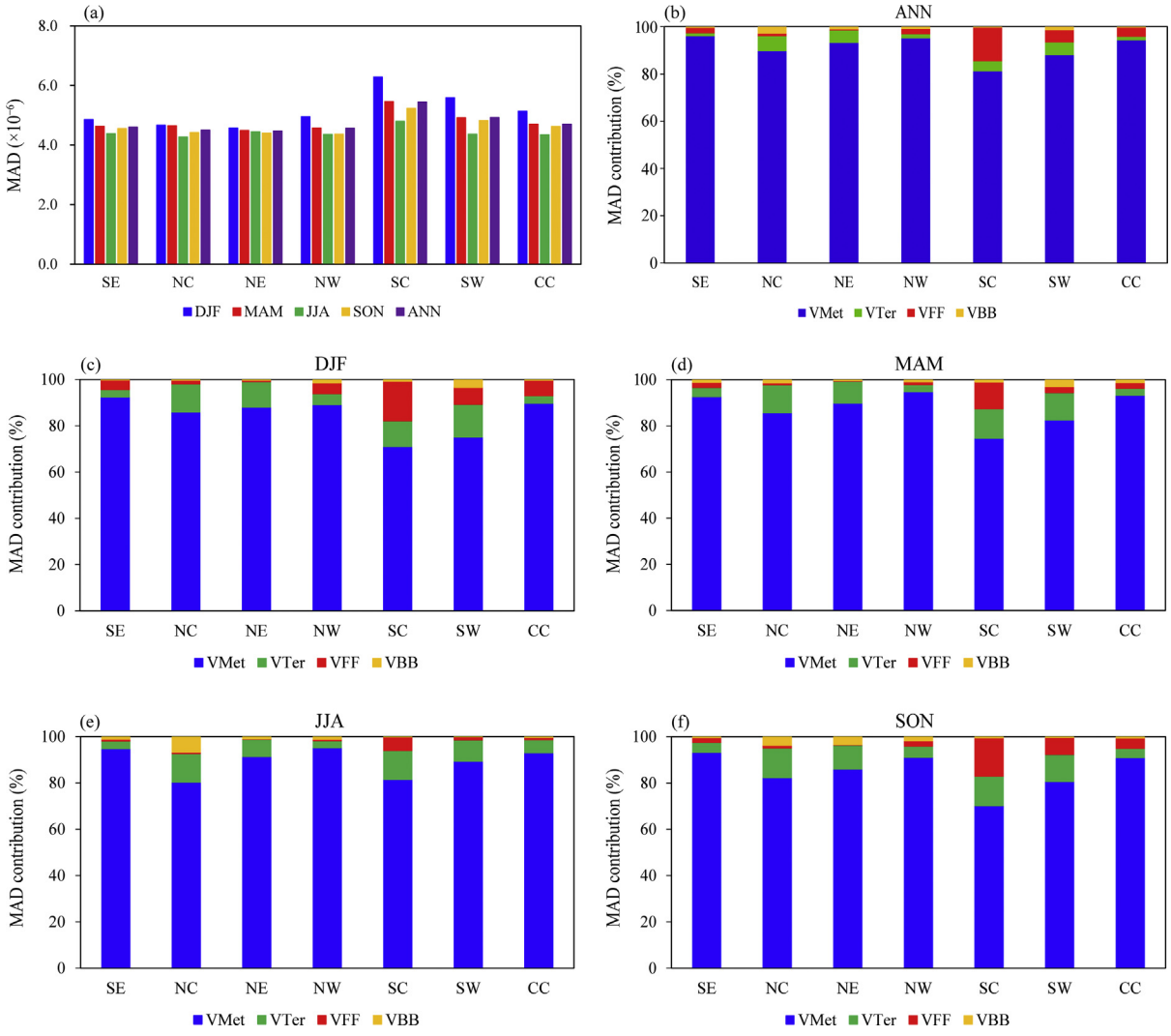

Fig. 7. The MAD values of seasonal and annual CO_2 concentrations from the simulation VAll (a); the MAD percentage contributions of annual and seasonal CO_2 concentration resulting from the variations of meteorological parameters alone (VMet), fossil fuel emissions alone (VFF), terrestrial fluxes alone (VTer) and biomass burning emissions alone (VBB) in each region of China (b–f).

respectively. It is found that the simulated surface CO_2 concentrations in VAll and VMet show similar variations, indicating that variations in meteorological parameters play a significant role in shaping the inter-annual variation of surface CO_2 concentration. The calculation shows that variations in meteorological parameters contribute 60%–85% to the inter-annual variation of the surface CO_2 concentration in different regions (Fig. 7b–f). And the contribution of terrestrial CO_2 fluxes is larger than the contribution of fossil fuel emissions to the inter-annual variations of the CO_2 concentration in North China, Northeast China, Northwest China and parts of southern China (e.g., Southwest China). In South China, the contribution of terrestrial CO_2 fluxes and the contribution of fossil fuel emissions to the CO_2 concentration are generally comparable in DJF, MAM and SON, while the variation of terrestrial CO_2 flux shows a larger contribution to the summertime CO_2 concentration than the variation of fossil fuel emissions. In general, variations in terrestrial fluxes and fossil fuel emissions may contribute up to 28% to the inter-annual variation of the CO_2 concentration in South China. The inter-annual variations of the CO_2 concentration due to variations of biomass burning emissions alone are generally smaller than those due to variations of terrestrial fluxes alone. However, the changes in biomass burning emissions might contribute as much as 7% to the inter-annual variation of the summertime CO_2 concentration in North China.

The inter-annual variations of the peaks-to-troughs amplitude are estimated as well. Fig. 8 presents the MAD and APDM values of the seasonal amplitude of the CO_2 concentration in VAll, VMet, VTer, VFF and VBB over different regions. Over 2004–2012, the APDM values of the seasonal amplitude for different regions in East Asia are within 11%–27% in VAll, with the largest inter-annual variation in the southern China (e.g. South China and Southwest China). The corresponding MAD values are within $(0.4–2.2) \times 10^{-6}$. The APDM of the CO_2 seasonal amplitude in VTer resembles that in VMet, reflecting that the effects of terrestrial flux variations

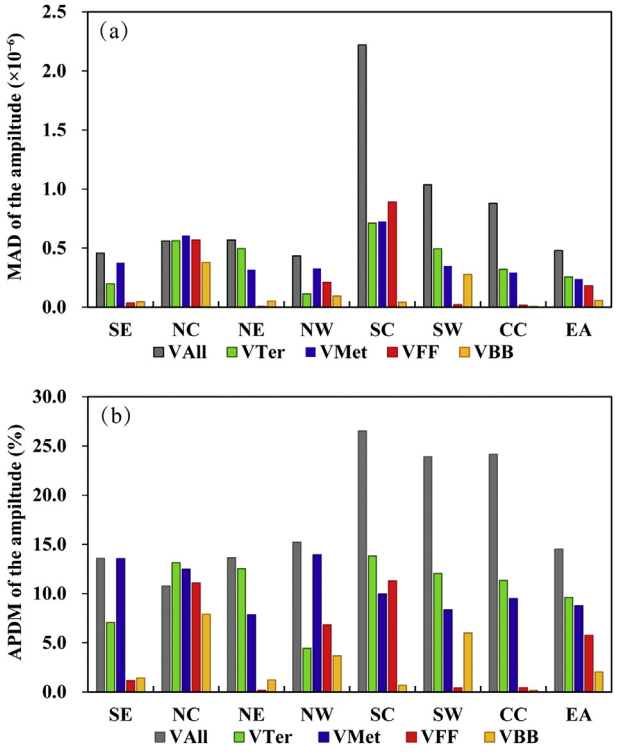

Fig. 8. The MAD (a) and the APDM (b) values of seasonal amplitudes of CO_2 concentrations from the simulation VAll, VTer, VMet, VFF and VBB averaged over studied domains.

alone on shaping the CO_2 amplitude could be comparable to the effects of meteorological parameters variations alone in most of studies regions. The influences of fossil fuel emissions are also found to be a significant contributor to forming the amplitude variation over the eastern China (e.g., North China and South China) where fossil fuel emissions are quite high. The APDM of the seasonal amplitude is about 11% owing to the inter-annual variations of fossil fuel emissions alone in South China and North China. The effects of the inter-annual variation in biomass burning could be more remarkable in local regions. For instance, in North China and Southwest China, the inter-annual variation of biomass burning emissions alone leads to a variation of ~6%−8% in the amplitude, while the variations of the seasonal amplitude in other regions are relatively insensitive to the variations of biomass burning emissions.

6. Conclusions and discussion

The spatiotemporal variations of surface CO_2 concentrations and the contributions of CO_2 sources and sinks on atmospheric CO_2 concentration in East Asia are investigated using the nested grid version of the global chemical transport model (GEOS-Chem) for the period of 2004−2012.

The comparisons of the model simulations with observations show that the model is reasonably skilled at reproducing the spatio-temporal (seasonal and annual) variations of atmospheric surface CO_2 concentrations in East Asia, but with an obvious overestimation of the summertime CO_2 concentration, which might be attributed to the higher uncertainties in terrestrial fluxes over East Asia. The model has poor performance at reproducing the observed peaks-to-troughs amplitude of atmospheric CO_2. The average seasonal amplitudes derived from simulations are roughly 50% or more lower than those from observations. The simulated surface CO_2 concentrations are generally increasing over East Asia during 2004−2012, with the overall trend of (2.0−3.0) $\times$ 10^{-6} per year. The inter-annual variations of the simulated surface CO_2 concentration averaged over East Asia are 4.6 $\times$ 10^{-6} for MAD and 1.2% for APDM. With meteorological parameters and prescribed CO_2 fluxes (fossil fuel emissions, biomass burning, terrestrial fluxes and oceanic fluxes) varying over 2004−2012, the inter-annual variation in the seasonal amplitude of the CO_2 concentration is about 15% for the APDM over East Asia.

The results indicate that variations in meteorological parameters play a crucial role in driving the inter-annual variations of the surface CO_2 concentration. However, the variations of the terrestrial fluxes alone and the variations of fossil fuel emissions alone also account for up to ~14% and ~17% of the inter-annual variation of the surface CO_2 concentration in local regions, respectively. The influences of biomass burning emissions contribute to ~7% of the inter-annual variation of the summertime CO_2 concentration in North China, while the influences in other regions are relatively small. It is found that the inter-annual variations of the seasonal amplitude of the CO_2 concentration are dependent on variations in both meteorological parameters and terrestrial fluxes. The inter-annual effects of fossil fuel emission variations on the seasonal amplitude are significant over South China and North China.

Nevertheless, many uncertainties remain in the spatial distribution of the terrestrial sources and sinks, particularly their temporal variations. Though the terrestrial fluxes from Carbon Tracker have been assessed with observations in some regions (e.g., North America), the uncertainties of terrestrial biosphere fluxes in East Asia still pose a challenge to the complete understanding of its impact on the inter-annual variations of CO_2 concentration over these regions. Moreover, besides the changes in vegetation growth and the corresponding CO_2 release and uptake, previous studies have suggested that the land-use activities such as deforestation and the intense agriculture may release carbon to the atmosphere, which could affect the variations of the CO_2 seasonal amplitude in the past several decades (IPCC, 2013; Zeng et al., 2014). Recently, it is reported that the current aerosol loading over China may affect the terrestrial carbon fluxes as well as the atmospheric CO_2 concentrations by diffuse radiation fertilization effect and hydrometeorological feedbacks (Xie et al., 2020), but these effects are not considered here. The large difference in the seasonal amplitude between simulation and observations also indicate that reducing the uncertainties in both model simulations and observations is challenging and needs further investigations.

Conflict of interest

The authors declare no conflict of interest.

Acknowledgments

This work was supported by the National Key Research and Development Program of China (2016YFA0600203), the National Natural Science Foundation of China (41977191 and 41405138), and the Major Programs of High−Resolution Earth Observation System (32-Y2-0A17-9001-15/17). We acknowledge Carbon Tracker product provided by NOAA ESRL, Boulder, Colorado, USA (http://carbontracker.noaa.gov). We express deep gratitude to all the research teams and providers for contributing their observation data to WDCGG (http://www.esa-ghg-cci.org/). We also acknowledge the research team for providing the CO_2 flux measurements on the ChinaFlux (http://www.chinaflux.org/index.aspx). We are very grateful to the NASA and the ACOS/OCO-2 project for the availability of GOSAT observations.

References

Chen, Z.H., Zhu, J., Zeng, N., 2013. Improved simulation of regional CO_2 surface concentrations using GEOS-Chem and fluxes from VEGAS. Atmos. Chem. Phys. 13 (15), 7607−7618.

CMA (China Meteorological Administration), 2018. China Greenhouse Gas Bulletin: the State of Greenhouse Gases in the Atmosphere Based on Chinese and Global Observations before 2017. http://www.cma.gov.cn/en2014/news/News/201901/P020190122575481732415.pdf.

Cogan, A.J., Boesch, H., Parker, R.J., et al., 2012. Atmospheric carbon dioxide retrieved from the Greenhouse gases Observing SATellite (GOSAT): comparison with ground-based TCCON observations and GEOS-Chem model calculations. J. Geophys. Res. 117 (D21). D21301.

Connor, B.J., Boesch, H., Toon, G., et al., 2008. Orbiting Carbon Observatory: inverse method and prospective error analysis. J. Geophys. Res. 113 (D5). D05305.

Corbett, J.J., Koehler, H.W., 2003. Updated emissions from ocean shipping. J. Geophys. Res. 108 (D20), 4650.

Corbett, J.J., Koehler, H.W., 2004. Considering alternative input parameters in an activity-based ship fuel consumption and emissions model: reply to comment by Øyvind Endresen et al. on "Updated emissions from ocean shipping". J. Geophys. Res. 109. D23303.

Deng, F., Chen, J.M., 2011. Recent global CO_2 flux inferred from atmospheric CO_2 observations and its regional analyses. Biogeosciences 8, 3263−3281.

Deng, F., Jones, D.B.A., Henze, D.K., et al., 2014. Inferring regional sources and sinks of atmospheric CO_2 from GOSAT XCO_2 data. Atmos. Chem. Phys. 14 (7), 3703−3727.

Deng, F., Jones, D.B.A., Walker, T.W., et al., 2015. Sensitivity analysis of the potential impact of discrepancies in stratosphere−troposphere exchange on inferred sources and sinks of CO_2. Atmos. Chem. Phys. 15, 11773−11788.

Feng, L., Palmer, P.I., Bösch, H., et al., 2009. Estimating surface CO_2 fluxes from space-borne CO_2 dry air mole fraction observations using an ensemble Kalman Filter. Atmos. Chem. Phys. 9, 2619−2633.

Feng, L., Palmer, P.I., Yang, Y., et al., 2011. Evaluating a 3-D transport model of atmospheric CO_2 using ground-based, aircraft, and space-borne data. Atmos. Chem. Phys. 11, 2789−2803.

Fu, Y., Liao, H., 2012. Simulation of the interannual variations of biogenic emissions of volatile organic compounds in China: impacts on tropospheric ozone and secondary organic aerosol. Atmos. Environ. 59, 170−185.

Fujita, D., Ishizawa, M., Maksyutov, S., et al., 2003. Inter-annual variability of the atmospheric carbon dioxide concentrations as simulated with global terrestrial biosphere models and an atmospheric transport model. Tellus B 55, 530−546.

IPCC, 2013. Climate Change 2013: the Physical Science Basis. Contribution of Working Group I to the Fifth Assessment Report of the Intergovernmental Panel on Climate Change. Cambridge University Press, Cambridge and New York.

Jiang, F., Chen, J.M., Zhou, L., et al., 2016. A comprehensive estimate of recent carbon sinks in China using both top-down and bottom-up approaches. Sci. Rep. 6, 22130.

Kou, X., Zhang, M., Peng, Z., et al., 2015. Assessment of the biospheric contribution to surface atmospheric CO_2 concentrations over East Asia with a regional chemical transport model. Adv. Atmos. Sci. 32, 287−300.

Kulawik, S., Wunch, D., O'Dell, C., et al., 2016. Consistent evaluation of ACOS-GOSAT, BESD-SCIAMACHY, CarbonTracker, and MACC through comparisons to TCCON. Atmos. Meas. Tech. 9, 683−709.

Lei, L.P., Guan, X.H., Zeng, Z.C., et al., 2014. A comparison of atmospheric CO_2 concentration GOSAT-based observations and model simulations. Sci. China Earth Sci. 57 (6), 1393−1402.

Le Quéré, C., Peters, G.P., Andres, R.J., et al., 2014. Global carbon budget 2013. Earth Syst. Sci. Data 6, 235−263.

Le Quéré, C., Andrew, R.M., Friedlingstein, P., et al., 2018. Global carbon budget 2017. Earth Syst. Sci. Data 10, 405−448.

Li, R., Zhang, M., Chen, L., et al., 2017. CMAQ simulation of atmospheric CO_2 concentration in East Asia: comparison with GOSAT observations and ground measurements. Atmos. Environ. 160, 176−185.

Lindqvist, H., O'Dell, C.W., Basu, S., et al., 2015. Does GOSAT capture the true seasonal cycle of carbon dioxide? Atmos. Chem. Phys. 15, 13023−13040.

Messerschmidt, J., Parazoo, N., Wunch, D., et al., 2013. Evaluation of seasonal atmosphere−biosphere exchange estimations with TCCON measurements. Atmos. Chem. Phys. 13, 5103−5115.

Miyazaki, K., Patra, P.K., Takigawa, M., et al., 2008. Global-scale transport of carbon dioxide in the troposphere. J. Geophys. Res. Atmos. 113, D15301.

Mu, Q., Liao, H., 2014. Simulation of the interannual variations of aerosols in China: role of variations in meteorological parameters. Atmos. Chem. Phys. 14, 9597−9612.

Nassar, R., Jones, D.B.A., Suntharalingam, P., et al., 2010. Modeling global atmospheric CO_2 with improved emission inventories and CO_2 production from the oxidation of other carbon species. Geosci. Model Dev. 3 (2), 689−716.

Nassar, R., Jones, D.B.A., Kulawik, S.S., et al., 2011. Inverse modeling of CO_2 sources and sinks using satellite observations of CO_2 from TES and surface flask measurements. Atmos. Chem. Phys. 11 (12), 6029−6047.

Nevison, C.D., Mahowald, N.M., Doney, S.C., et al., 2008. Contribution of ocean, fossil fuel, land biosphere, and biomass burning carbon fluxes to seasonal and interannual variability in atmospheric CO_2. J. Geophys. Res. Biogeosci. 113 https://doi.org/10.1029/2007JG000408. G01010.

Oda, T., Maksyutov, S., 2011. A very high-resolution (1 km x 1 km) global fossil fuel CO_2 emission inventory derived using a point source database and satellite observations of nighttime lights. Atmos. Chem. Phys. 11, 543−556.

Olsen, S.C., Brasseur, G.P., Wuebbles, D.J., et al., 2013. Comparison of model estimates of the effects of aviation emissions on atmospheric ozone and methane. Geophys. Res. Lett. 40 (22), 6004−6009.

Osterman, G., Eldering, A., Cheng, C., et al., 2017. ACOS Level 2 Standard Product and Lite Data Product Data User's Guide, v7.3. NASA GES DISC, Pasadena, CA, USA. https://docserver.gesdisc.eosdis.nasa.gov/public/project/OCO/ACOS%20v7.3_DataUsersGuide-RevE.pdf.

Peters, W., Jacobson, A.R., Sweeney, C., et al., 2007. An atmospheric perspective on North American carbon dioxide exchange: CarbonTracker. Proc. Natl. Acad. Sci. U. S. A. 104 (48), 18925−18930.

Piao, S., Ciais, P., Friedlingstein, P., et al., 2009a. Spatiotemporal patterns of terrestrial carbon cycle during the 20th century. Global Biogeochem. Cycles 23, GB4026.

Piao, S., Fang, J., Ciais, P., et al., 2009b. The carbon balance of terrestrial ecosystems in China. Nature 458, 1009−1013.

Poulter, B., Frank, D., Ciais, P., et al., 2014. Contribution of semi-arid ecosystems to interannual variability of the global carbon cycle. Nature 509, 600−603.

Randerson, J.T., Thompson, M.V., Conway, T.J., et al., 1997. The contribution of terrestrial sources and sinks to trends in the seasonal cycle of atmospheric carbon dioxide. Global Biogeochem. Cycles 11, 535−560.

Shim, C.S., Nassar, R., Kim, J., 2011. Comparison of model-simulated atmospheric carbon dioxide with GOSAT retrievals. Asian J. Atmos. Environ. 5, 263−277.

Simone, N.W., Stettler, M.E.J., Barrett, S.R.H., 2013. Rapid estimation of global civil aviation emissions with uncertainty quantification. Transp. Res. Part D 25, 33−41.

Sitch, S., Friedlingstein, P., Gruber, N., et al., 2015. Recent trends and drivers of regional sources and sinks of carbon dioxide. Biogeosciences 12 (3), 653−679.

Suntharalingam, P., Jacob, D.J., Palmer, P.I., et al., 2004. Improved quantification of Chinese carbon fluxes using CO_2/CO correlations in Asian outflow. J. Geophys. Res. Atmos. 109. D18S18.

Takahashi, T., Sutherland, S.C., Wanninkhof, R., et al., 2009. Climatological mean and decadal change in surface ocean pCO_2, and net sea−air CO_2 flux over the global oceans. Deep Sea Res. Part II Top. Stud. Oceanogr. 56 (8−10), 554−577.

Thompson, R.L., Patra, P.K., Chevallier, F., et al., 2016. Top−down assessment of the Asian carbon budget since the mid-1990s. Nat. Commun. 7, 10724.

van der Werf, G. R., Randerson, J. T., Giglio, L., et al., 2010. Global fire emissions and the contribution of deforestation, savanna, forest, agricultural, and peat fires (1997−2009). Atmos. Chem. Phys. 10, 11707−11735.

Wang, J., Zeng, N., Wang, M., 2016. Interannual variability of the atmospheric CO_2 growth rate: roles of precipitation and temperature. Biogeosciences 13, 2339−2352.

Wunch, D., Toon, G.C., Blavier, J.F.L., et al., 2011a. The total carbon column observing network. Phil. Trans. R. Soc. Lond. A Math. Phys. Eng. Sci. 369, 2087−2112.

Wunch, D., Wennberg, P.O., Toon, G.C., et al., 2011b. A method for evaluating bias in global measurements of CO_2 total columns from space. Atmos. Chem. Phys. 11, 12317−12337.

Xie, X., Wang, T., Yue, X., et al., 2020. Effects of atmospheric aerosols on terrestrial carbon fluxes and CO_2 concentrations in China. Atmos. Res. 237, 104859.

Yevich, R., Logan, J.A., 2003. An assessment of biofuel use and burning of agricultural waste in the developing world. Global Biogeochem. Cycles 17 (4), 1095. https://doi.org/10.1029/2002GB001952.

Yu, G.R., Wen, X.F., Sun, X.M., et al., 2006a. Overview of ChinaFLUX and evaluation of its eddy covariance measurement. Agric. For. Meteorol. 137, 125−137.

Yu, G.R., Fu, Y., Sun, X., et al., 2006b. Recent progress and future direction of ChinaFLUX. Sci. China Ser. D 49 (Suppl. II), 1−23.

Yu, G.R., Zhang, L.M., Sun, X.M., et al., 2008. Environmental controls over carbon exchange of three forest ecosystems in eastern China. Global Change Biol. 14, 2555−2571.

Yu, G.R., Zhu, X.J., Fu, Y.L., et al., 2013. Spatial patterns and climate drivers of carbon fluxes in terrestrial ecosystems of China. Global Change Biol. 19 (3), 798−810.

Zeng, N., Mariotti, A., Wetzel, P., 2005. Terrestrial mechanisms of interannual CO_2 variability. Global Biogeochem. Cycles 19, GB1016.

Zeng, N., Zhao, F., Collatz, G.J., et al., 2014. Agricultural Green Revolution as a driver of increasing atmospheric CO_2 seasonal amplitude. Nature 515, 394−397.

Zhang, H.F., Chen, B.Z., Machida, T., et al., 2014. Estimating Asian terrestrial carbon fluxes from CONTRAIL aircraft and surface CO_2 observations for the period 2006-2010. Atmos. Chem. Phys. 14 (11), 5807−5824.

Zhang, H.F., Chen, B.Z., Xu, G., et al., 2015. Comparing simulated atmospheric carbon dioxide concentration with GOSAT retrievals. Sci. Bull. 60, 380−386.